Challenges and structural characterization of the solid solution $Cu_2Zn(Ge_xSi_{1-x})Se_4$

Sara Niedenzu[1,2], Galina Gurieva[1], and Susan Schorr[1,2]

[1]Helmholtz-Zentrum Berlin für Materialien und Energie, Berlin, Berlin, Hahn-Meitner-Platz 1, Germany
[2]Freie Universität Berlin, Berlin, Berlin, Malteserstr. 74, Germany

***Abstract* — The quaternary chalcogenides $Cu_2ZnSiSe_4$ and $Cu_2ZnGeSe_4$ crystallize in the orthorhombic wurtz-stannite and tetragonal kesterite type structures, respectively. To investigate the structural transformation within the solid solution series $Cu_2Zn(Ge_xSi_{1-x})Se_4$ a systematic structural study was performed. Polycrystalline samples, prepared by solid state reaction, show a single quaternary phase as analyzed by WDX spectroscopy. Structural parameters of the mixed crystals were obtained using powder X-ray diffraction. It can be shown that apart from $Cu_2ZnSiSe_4$, Si-rich mixed crystals of this series adopt the wurtz-stannite type structure. The lattice parameters are in consistency with Vegard's law and increase with increasing Ge content.**

***Index Terms* — $Cu_2ZnSiSe_4$, $Cu_2ZnGeSe_4$, polycrystalline powders, X-Ray diffraction, chalcogenides, semiconductor alloys.**

I. Introduction

The quaternary chalcogenide semiconductors Cu_2-B^{II}-C^{IV}-X_4 (B^{II}-Zn; C^{IV}-Ge, Si, X-S, Se) contain only earth abundant, non-toxic elements and have drawn wide attention for their potential applications in many fields. Depending on their band gaps these materials are interesting for thin film solar cells [1,2], high-temperature thermoelectric materials [3], and non-linear optics [4]. For instance $Cu_2ZnGeSe_4$ is a promising candidate for top cell absorber layers in multi junction solar cells due to its band gap of 1.5 eV [1]. Moreover they are interesting as thermoelectric materials [3]. The band gap can be tuned by different anion ratios such as in the solid solution $Cu_2ZnGe(S_{1-x}Se_x)_4$. However due to challenges in controlling the anion ratio, cationic substitution like Ge ↔ Si, as in this study, is considered as alternative method in order to perform band gap engineering. Thus $Cu_2ZnSiSe_4$, which has a band gap of 2.2 eV [5], is proven to be a promising nonlinear optical material for use in the infrared region [4].

For the design of materials the structure-property relationship is a key feature, which requires crystallographic background. Experimental and theoretical studies show that $Cu_2ZnGeSe_4$ crystallizes in the kesterite type structure (space group $I\bar{4}$) [6, 7], which is also predicted to be the ground state structure for this material [8]. The experimental results are based on neutron diffraction data [6]. Based on powder X-ray diffraction data, $Cu_2ZnSiSe_4$ crystallizes in the orthorhombic wurtz-stannite type structure (space group $Pmn2_1$) [9].

However the structural transformation in the solid solution $Cu_2Zn(Ge_xSi_{1-x})Se_4$ from the orthorhombic end member $Cu_2ZnSiSe_4$ (space group $Pmn2_1$) to the tetragonal end member $Cu_2ZnGeSe_4$ (space group $I\bar{4}$) is not clear. The question arises at which composition x the crystal structure changes from the orthorhombic wurtz-stannite type structure to the tetragonal kesterite type structure or if there is a miscibility gap. By now no experimental results for the solid solution $Cu_2Zn(Ge_xSi_{1-x})Se_4$ are reported in the literature to clarify these questions. In this study structural insights into the solid solution $Cu_2Zn(Ge_xSi_{1-x})Se_4$ over the full composition range of x = 0 - 1 will be given.

II. Experimental

Polycrystalline powders of the $Cu_2Zn(Ge_xSi_{1-x})Se_4$ solid solution were synthesized by solid state reaction from the pure elements Cu, Zn, Ge, Si, and Se. The weighted elements were placed in a graphite boat and sealed in evacuated silica tubes, which were placed in the furnace and heated up until 900 °C (x = 0 – 0.4) and 840 °C (x = 0.5 – 1) with a heating rate of 10 K/h for the reaction step. The maximum temperatures were hold for 300h. The different temperatures were chosen to stay below the melting point of the quaternary compound, therefore different maximum temperatures were selected depending on the Ge:Si cation ratio. Interstitial steps at 250 °C (48 h), 450 °C (48 h), and 650 °C (48 h) were introduced to avoid explosion due to the partial pressure of Se. The samples were cooled down to room temperature with a cooling rate of 10 K/h. In a following step the samples were homogenized by grinding them in an agate mortar and pressed to pellets. The pellets were annealed in evacuated silica tubes in the furnace for 300 h at the same temperatures as chosen for the reaction step with a heating rate of 50 K/h. Cooling followed with a cooling rate of 10 K/h.

The chemical homogeneity and chemical composition of the synthesized polycrystalline powders were proven by wavelength dispersive X-ray spectroscopy (WDX) using an electron microprobe of the type JEOL JXA 8200 Superprobe. The quantitative element analysis includes an error of 2 %. 35 grains per sample were measured with 10 measurement points per grain performed by a line scan. The chemical composition of a phase was averaged over 35 grains.

Basic structural information and phase analysis were determined on the basis of X-ray powder diffraction data. The measurements of the polycrystalline powders were performed at a Panalytical X'Pert Pro MPD using Bragg-Brentano geometry with a focusing beam and Cu-$K\alpha_{(1+2)}$ radiation. As instrumental setup a sample spinner, ¼ divergence slit, and a 5mm mask were chosen. The measurements were performed over a 2θ range from 10° to 130° with steps of 0.013° and a step time of 100s.

III. RESULTS AND DISCUSSION

Back scattered electron (BSE) images (Fig. 1) taken at the electron microprobe show that the samples of the solution present a homogenous quaternary phase alongside with hardly distinct secondary phases. The secondary phases observed are ZnSe and copper selenides, while Cu appears in different oxidation states (CuSe, Cu_2Se, Cu_3Se_2). Cu is partially substituted by Si in all copper selenides (e.g. $Cu_{1-y}Si_ySe$).

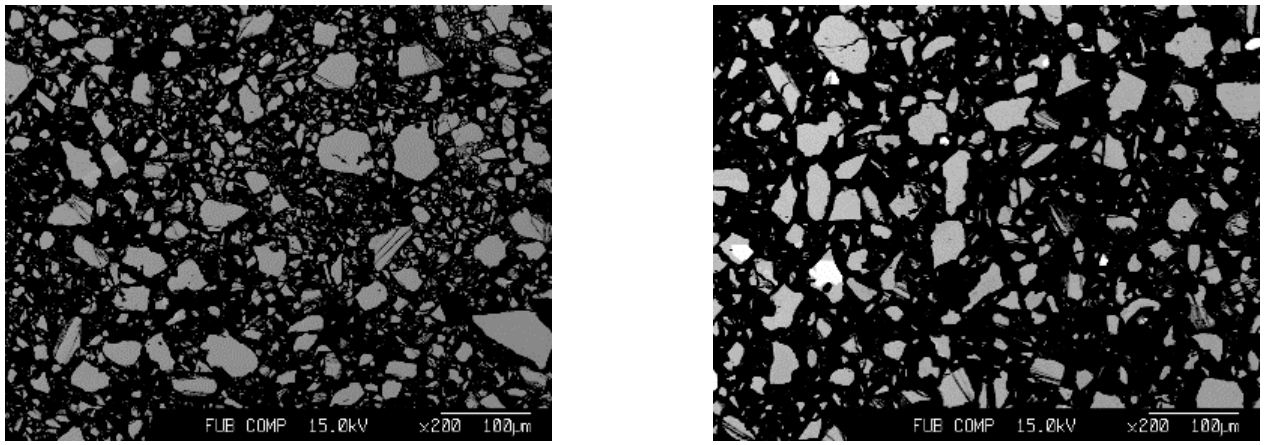

Fig. 1: BSE image of $Cu_2ZnSiSe_4$ (left, grey: $Cu_2ZnSiSe_4$, black: epoxy matrix) and $Cu_2Zn(Ge_{0.28}Si_{0.74})Se_4$ (right, grey: $Cu_2Zn(Ge_{0.28}Si_{0.74})Se_4$, white: $Cu_{0.3}Si_{0.4}Se$, black: epoxy matrix)

The chemical analysis showed that each sample of $Cu_2Zn(Ge_xSi_{1-x})Se_4$ with x = 0 – 1 contains only one quaternary phase. While the samples with x = 0 – 0.37 are slightly Cu and Zn poor (Fig. 2), samples with x = 0.58 – 1 are Cu and Zn rich (Fig. 2).

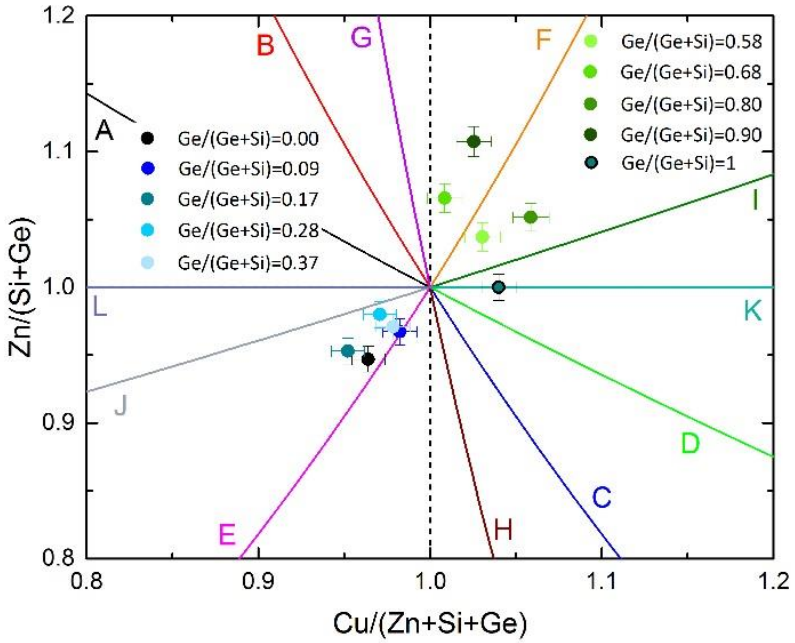

Fig. 2: Cation ratio plot Cu/(Zn+Si+Ge) vs. Zn/(Si+Ge) showing the different off-stoichiometric types.

For the visualization of the off-stoichiometric composition of $Cu_2Zn(Ge_xSi_{1-x})Se_4$ mixed crystals the cation ratio plot indicating the off-stoichiometry types (A – L) [7] was used. All Si-rich $Cu_2Zn(Ge_xSi_{1-x})Se_4$ mixed crystals plot within the J-E-type field. Except for one sample, the $Cu_2Zn(Ge_xSi_{1-x})Se_4$ mixed crystals with increasing Ge/(Ge+Si) ratio tend to move towards the stoichiometric point (Fig. 2). In Ge-rich $Cu_2Zn(Ge_xSi_{1-x})Se_4$ mixed crystals the cation ratios are more widespread and the samples plot within the G-F-type field, the F-I-type field, and on the line of the K-type (Fig. 2). $Cu_2Zn(Ge_xSi_{1-x})Se_4$ mixed crystals with lower Ge/(Ge+Si) ratio plot closer to the stoichiometric point, whereas mixed crystals with higher Ge/(Ge+Si) ratios are getting more off-stoichiometric (Fig. 2).

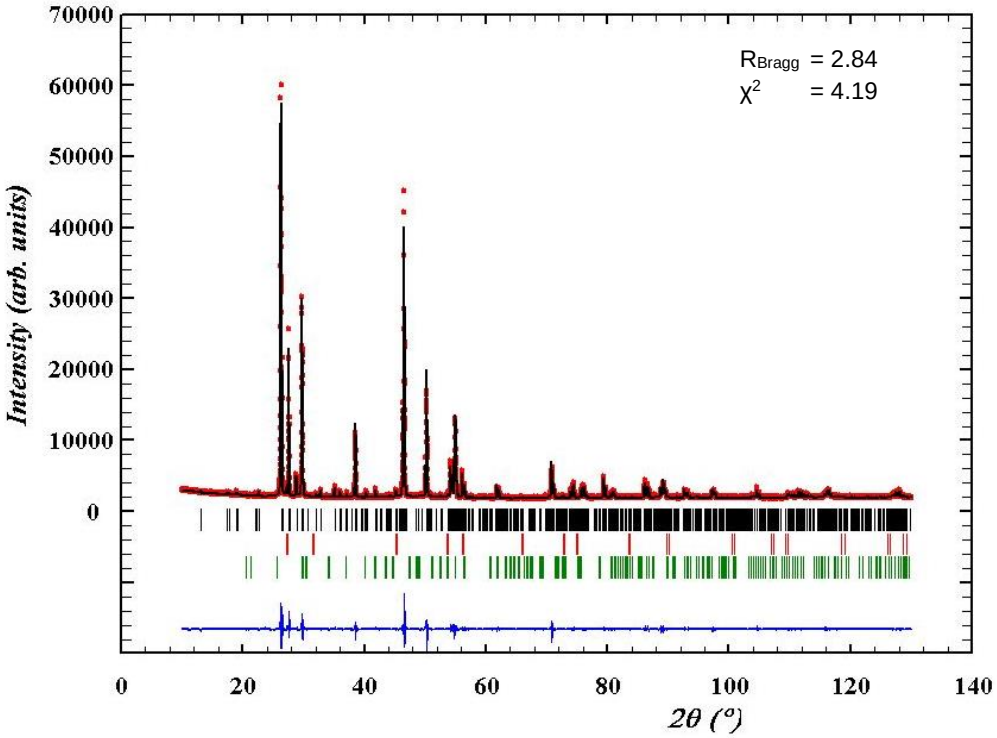

Fig. 3: Le Bail refinement of X-ray diffraction data of $Cu_2ZnSiSe_4$, using the wurtz-stannite structure model. Experimental data are shown by the red dots, the obtained fit is the black line, the refined phase reflections of the quaternary phase $Cu_2ZnSiSe_4$ are the black ticks, ZnSe the red ticks, $Cu_{3-y}Si_ySe_2$ the green ticks and the difference between experimental and fitted data is the blue line.

The deviation from the stoichiometry in the $Cu_2Zn(Ge_xSi_{1-x})Se_4$ mixed crystals can be explained by the presence of the secondary phases ZnSe, and copper selenides but also by the volatility of Ge. In the Si-rich $Cu_2Zn(Ge_xSi_{1-x})Se_4$ with x = 0 – 37 the volatility of Ge plays a less pronounced role than in the Ge-rich mixed crystals due to the lower content of Ge. However, in all Si-rich samples the secondary phases ZnSe and copper selenides along with Si are present. In the end member $Cu_2ZnSiSe_4$, binary $Cu_{3-y}Si_ySe$ could have been observed, and in the rest of the Si-rich samples, $Cu_{1-y}Si_ySe$ is present. The Si-rich binaries $Cu_{1-y}Si_ySe$ are present in the samples with increasing Ge/(Ge+Si) ratios for which the composition of the mixed crystals move into the direction of the J-type line (Fig. 2). Samples with lower Ge/(Ge+Si) ratios contain Cu-rich binaries, here the mixed crystals plot closer to the E-type line (Fig. 2). In all Ge-rich samples (x = 0.58 – 0.9) the binaries ZnSe and $Cu_{2-y}Si_ySe$ could have been observed. $Cu_{2-y}Si_ySe$ seem to be pronounced in the same degree in all Ge-rich samples, however ZnSe is more distinct in two of the samples. In these samples the $Cu_2Zn(Ge_xSi_{1-x})Se_4$ mixed crystals plot within the F-I-type field (Fig. 2). Mixed crystals with lower Ge/(Ge+Si) ratios are closer to the stoichiometric point than the samples with higher Ge/(Ge+Si) ratios (Fig. 2). The shift away from the stoichiometric point with increasing Ge/(Ge+Si) ratios can be explained by the loss of Ge due to its volatility (Fig. 2). Hence difficulties in controlling the loss of Ge due to its volatility may also explain the widespread cation ratios of $Cu_2Zn(Ge_xSi_{1-x})Se_4$ with x = 0.58 – 1 (Fig. 2). The loss of Ge during the synthesis steps has already been observed in polycrystalline powders of the end member $Cu_2ZnGeSe_4$ [7].

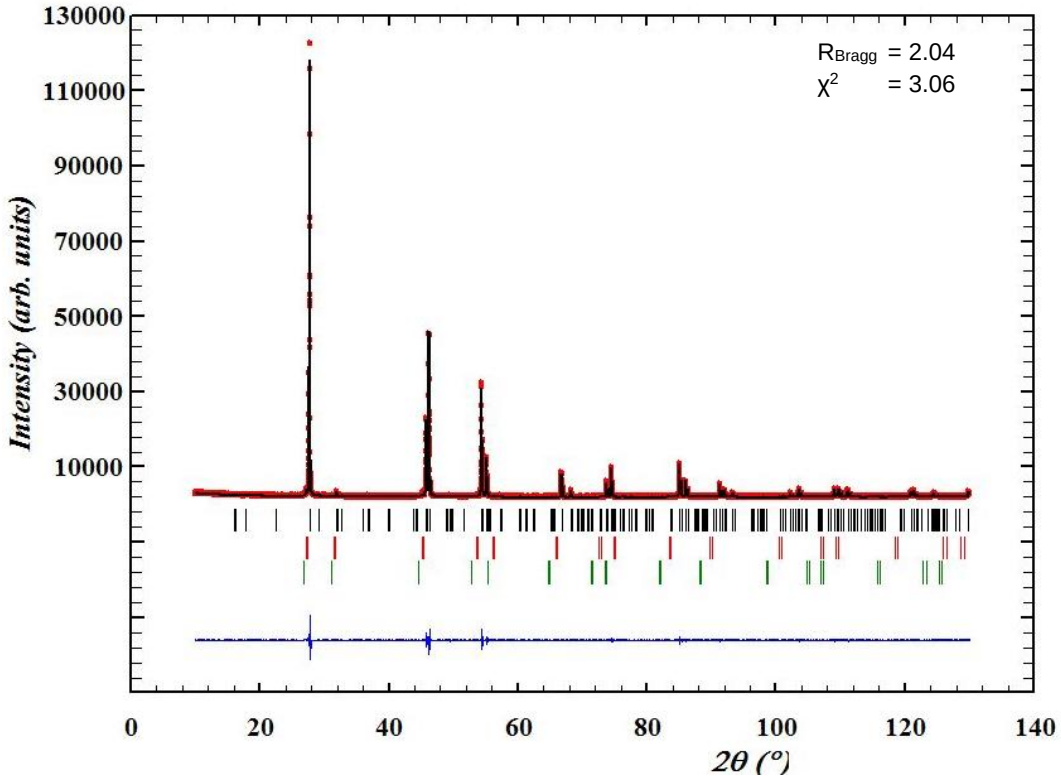

Fig. 4: Le Bail refinement of X-ray diffraction data of $Cu_2Zn(Ge_{0.58}Si_{0.39})Se_4$, using the kesterite structure model. Experimental data are shown by the red dots, the obtained fit is the black line, the refined phase reflections of the quaternary phase $Cu_2Zn(Ge_{0.58}Si_{0.39})Se_4$ are the black ticks, ZnSe the red ticks, $Cu_{2-y}Si_ySe$ the green ticks and the difference between experimental and fitted data is the blue line.

According to the crystal structure refinement of powder X-ray diffraction data the end member $Cu_2ZnSiSe_4$ adopts the orthorhombic wurtz-stannite type structure (space group $Pmn2_1$) with a = 7.827 Å, b = 6.733 Å, and c = 6.453 Å (Fig. 3). These results are in good agreement with previously reported values, obtained from X-ray diffraction of polycrystalline powders and single crystals of $Cu_2ZnSiSe_4$ [9]. Also the Si-rich mixed crystals of $Cu_2Zn(Ge_xSi_{1-x})Se_4$ with x = 0.09 – 0.37 adopt the orthorhombic wurtz-stannite type structure (space group $Pmn2_1$). In contrast the end member $Cu_2ZnGeSe_4$ adopts the tetragonal kesterite type structure (space group $I\bar{4}$) with a = 5.612 Å, and c = 11.041 Å, which has already been reported in a neutron diffraction study [6]. These values are also in good agreement with further reported results of off-stoichiometric polycrystalline powder of $Cu_2ZnGeSe_4$ [7]. The Ge-rich $Cu_2Zn(Ge_xSi_{1-x})Se_4$ mixed crystals with x = 0.58 – 0.9 adopt the tetragonal stannite or kesterite type structure (space groups $I\bar{4}2m$ and $I\bar{4}$, respectively). The stannite and kesterite type structure distinguish by a different cation layering [10]. Whereas in the kesterite type structure CuZn layers alternate with CuGe layers, in the stannite type structure Cu_2 layers alternate with ZnGe layers [10]. These two structure types cannot be distinguished by X-ray diffraction since Cu^+, Zn^{2+}, and Ge^{4+} are isoelectronic cations and have a similar scattering power for X-rays. However by using neutron diffraction it is possible to distinguish the Cu^+, Zn^{2+}, and Ge^{4+} cations, since they show different neutron scattering lengths and thus to differentiate between the tetragonal kesterite and stannite type structure and between Cu^+ and Zn^{2+} in the wurtz-stannite type structure. Lattice parameters of the $Cu_2Zn(Ge_xSi_{1-x})Se_4$ mixed crystals resulted from Le Bail refinement using the wurtz-stannite type structure (space group $Pmn2_1$) for $0.0 < x \geq 0.37$ and using the kesterite type structure (space group $I\bar{4}$) for $0.58 \leq x > 1$ as starting model. The kesterite type structure was chosen (space group $I\bar{4}$) instead of the stannite type structure (space groups $I\bar{4}2m$) for the Ge-rich samples since for the end member $Cu_2ZnGeSe_4$ the kesterite type structure was already confirmed by neutron diffraction [6, 7].

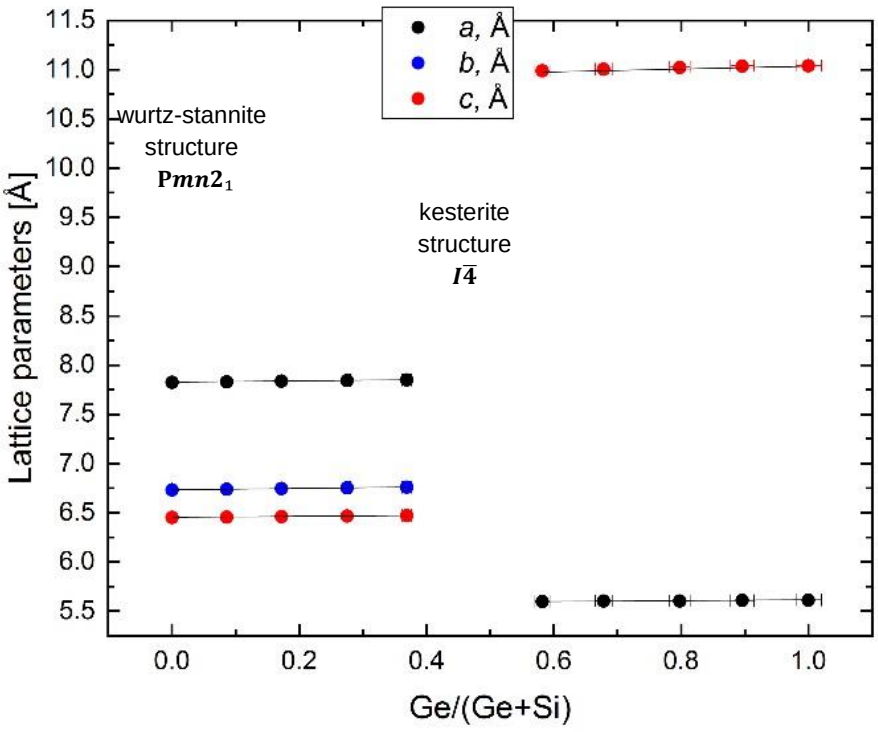

Fig. 5: The plot shows lattice parameters of $Cu_2Zn(Ge_xSi_{1-x})Se_4$ with x = 0 - 0.37, 0.58 - 1 (gained by Le Bail analysis of XRD data) versus the cation ratio Ge/(Ge+Si). The lines are a guide for the eye.

The obtained lattice parameters of the $Cu_2Zn(Ge_xSi_{1-x})Se_4$ solid solution are shown in Tab. 1. It can be observed that with an increasing Ge content the lattice parameters also increase slightly. This behavior is present in both the orthorhombic and the tetragonal mixed crystals. This behavior could already been observed by a visual inspection of the XRD pattern in which the main peaks were shifted into the direction of smaller 2θ angles with an increasing amount of Ge. The lattice parameters of orthorhombic $Cu_2Zn(Ge_xSi_{1-x})Se_4$ (x = 0 – 0.37) and tetragonal $Cu_2Zn(Ge_xSi_{1-x})Se_4$ (x = 0.58 – 1) are in good agreement with Vegard's law (Fig. 5). However it is still a challenge to understand the structural transition from the orthorhombic to the tetragonal crystal structure (Fig. 5). The gap between x = 0.45 – 0.55 in $Cu_2Zn(Ge_xSi_{1-x})Se_4$ remains an open question and will be investigated further.

TABLE I

STRUCTURAL PARAMETERS OF THE REFINED DATA FROM THE EXPERIMENTAL RESULTS OF $Cu_2Zn(Ge_xSi_{1-x})Se_4$

Sample	Unit Cell Parameters			Further Crystallographic Information		
	a [Å]	*b* [Å]	*c* [Å]	crystal system	crystal structure	space group
$Cu_{1.93}Zn_{0.97}Si_{1.03}Se_4$	7.827	6.733	6.453	orthorhombic	wurtz-stannite	$Pmn2_1$
$Cu_{1.97}Zn_{0.98}(Ge_{0.09}Si_{0.93})Se_4$	7.831	6.739	6.457	orthorhombic	wurtz-stannite	$Pmn2_1$
$Cu_{1.92}Zn_{0.98}(Ge_{0.17}Si_{0.85})Se_4$	7.839	6.747	6.462	orthorhombic	wurtz-stannite	$Pmn2_1$
$Cu_{1.96}Zn_{0.99}(Ge_{0.28}Si_{0.74})Se_4$	7.843	6.753	6.467	orthorhombic	wurtz-stannite	$Pmn2_1$
$Cu_{1.95}Zn_{0.99}(Ge_{0.37}Si_{0.65})Se_4$	7.850	6.760	6.472	orthorhombic	wurtz-stannite	$Pmn2_1$
$Cu_{2.05}Zn_{1.02}(Ge_{0.58}Si_{0.39})Se_4$	5.599	–	10.991	tetragonal	stannite/kesterite	$I\bar{4}2m/I\bar{4}$
$Cu_{2.03}Zn_{1.04}(Ge_{0.68}Si_{0.30})Se_4$	5.604	–	11.007	tetragonal	stannite/kesterite	$I\bar{4}2m/I\bar{4}$
$Cu_{2.10}Zn_{1.02}(Ge_{0.80}Si_{0.19})Se_4$	5.603	–	11.024	tetragonal	stannite/kesterite	$I\bar{4}2m/I\bar{4}$
$Cu_{2.06}Zn_{1.06}(Ge_{0.90}Si_{0.06})Se_4$	5.610	–	11.038	tetragonal	stannite/kesterite	$I\bar{4}2m/I\bar{4}$
$Cu_{2.05}Zn_{0.99}Ge_{0.99}Se_4$	5.612	–	11.041	tetragonal	kesterite	$I\bar{4}$

IV. SUMMARY

The chemical analysis of the polycrystalline solid solution series $Cu_2Zn(Ge_xSi_{1-x})Se_4$ with $0 \leq x \geq 0.37$ as well as $0.58 \leq x \geq 1$ was performed by WDX spectroscopy using an electron microprobe analysis system. All Si-rich as well as Ge-rich mixed crystals show one quaternary $Cu_2Zn(Ge_xSi_{1-x})Se_4$ phase. Additionally secondary phases like ZnSe and copper selenides along with substitutional Si has been obtained. The structural properties of the mixed crystals were investigated by X-ray diffraction. For $Cu_2Zn(Ge_xSi_{1-x})Se_4$ with $0 \leq x \geq 0.37$ the wurtz-stannite type structure (space group $Pmn2_1$) has been established. However the Ge-rich side of the solid solution adopt the stannite type structure (space group $I\bar{4}2m$) or the kesterite type structure (space group $I\bar{4}$). The end member $Cu_2ZnGeSe_4$ crystallizes in the tetragonal kesterite type structure. For the end member $Cu_2ZnSiSe_4$ and $Cu_2ZnGeSe_4$ the lattice parameters are in good agreement with previous experimental results. The lattice parameters of both, orthorhombic as well as tetragonal mixed crystals, are in good agreement with Vegard's law. It is the first time that $Cu_2Zn(Ge_xSi_{1-x})Se_4$ mixed crystals with a composition close to the structural transition have been synthesized. The gap between $0.45 \leq x \geq 0.55$ remains an open question and will be investigated further.

ACKNOWLEDGEMENTS

Financial supports gained from HZB Graduate School MatSEC (Materials for Solar Energy Conversion). Furthermore, the research leading to the presented results has been partially supported by the STARCELL project as well as INFINITE-CELL project. These projects have received funding from the European Union's Horizon 2020 research and innovation programme under the Marie Skłodowska-Curie grant agreements No 720907 and 777968 respectively.

REFERENCES

[1] T. Schnabel, M. Seboui, and E. Ahlswede, "Band gap tuning of $Cu_2ZnGeS_xSe_{4-x}$ absorbers for thin-film solar cells," *Energies*, vol. 10, pp. 1813-1822, 2017.

[2] Q. Guo, G.M. Ford, W.-C. Yang, C.J .Hages, H.W. Hillhouse, and R. Agrawal, "Enhancing the performance of CZTSSe solar cells with Ge alloying," *Solar Energy Materials & Solar Cells*, vol. 105, pp. 132-136, 2012.

[3] C. P. Heinrich, T.W. Day, W.G. Zeier, G.J. Snyder, and W. Tremel, "Effect of isovalent substitution on the thermoelectric properties of the $Cu_2ZnGeSe_{4-x}S_x$ series of solid solutions", *Journal of the American Chemical Society*, vol. 136, pp. 442−448, 2014.

[4] K.A. Rosmus J.A. Brant, S.D. Wisneski, D.J. Clark, Y.S. Kim, J.I. Jang, C.D. Brunetta, J.-H. Zhang, M.N. Srnec, and J.A. Aitken, "Optical nonlinearity in Cu_2CdSnS_4 and α/β-Cu_2ZnSiS_4: diamond-like semiconductors with high laser-damage thresholds," *Inorganic Chemistry*, vol. 53, pp. 7809−781, 2014.

[5] G.-Q. Yao, H.-S. Shen, E.D. Honig, R. Kershaw, K. Dwigh, and A. Wold, "Preparation and characterization of the quaternary chalcogenides Cu_2(BII)C(IV)X_4 [B(II) = Zn, Cd; C(IV) = Si, Ge, X = S, Se]," *Solid State Ionics*, vol. 24, pp. 249–252, 1987.

[6] G. Gurieva, D.M. Többens, M. Ya. Valakh, and S. Schorr, Cu-Zn disorder in $Cu_2ZnGeSe_4$, "A complementary neutron diffraction and Raman spectroscopy study," *Journal of Physics and Chemistry of Solids*, vol. 99, pp. 100-104, 2016.

[7] R. Gunder, J. A. Márquez-Prieto, G. Gurieva, T. Unold, and S. Schorr, "Structural characterization of off-stoichiometric kesterite-type $Cu_2ZnGeSe_4$ compound semiconductors: from cation distribution to intrinsic point defect density," *CrystEngComm*, vol. 20, pp. 1465–1604, 2018.

[8] S. Chen, A. Walsh, Y. Luo, J.H. Yang, X.G. Gong, S.H. Wei, "Wurtzite-derived polytypes of kesterite and stannite quaternary chalcogenide semiconductors," *Physical Review B*, vol. 82, pp. 195203-195211, 2010.
[9] G. Gurieva, S. Levcenko, V.Ch. Kravtsov, A. Nateprov, E. Irran, Y.-S. Huang, E. Arushanov, and S. Schorr, "X-ray diffraction investigation on $Cu_2ZnSiSe_4$ single and polycrystalline crystals," *Zeitschrift Kristallographie*, pp. 1828-183, 2015
[10] S. Schorr, "The crystal structure of kesterite type compounds: A neutron and X-ray diffraction study," *Solar Energy Materials & Solar Cells*, pp. 1482–1488, 2011